Executive Summary

This manual summarizes the theory and preliminary verifications of the Vortex Step Method (VSM) module (Kite-VSM (KiteVSM)), which is part of Kite-AeroDyn (KiteAD), the new aerodynamics module of Kite-FAST (Kite-FAST) for airborne wind energy. SOMETHING ABOUT THEORY AND VERIFICATION HERE. The results are encouraging, and future improvements to the code are recommended in this manual.

Acknowledgments

This work was supported by Makani Google X under Contract No. with the National Renewable Energy Laboratory.

Table of Contents

Acronyms . . . vi
Greek Symbols . . . vi

1 Overview . . . 1
1.1 VSM Theory Development . . . 1
1.2 Kite-VSM (KiteVSM) additional theory . . . 7

2 Implementation Algorithm . . . 8
2.1 Inputs, Outputs, Parameters, States . . . 8
2.1.1 Init_Inputs . . . 8
2.2 Inputs u . . . 8
2.3 Outputs y . . . 8
2.4 States x_z . . . 9
2.5 Parameters p . . . 9
2.6 Kite-VSM Implementation . . . 9
2.6.1 KiteVSM_Init Routine . . . 9
2.6.2 KiteVSM_UpdateStates Routine . . . 9
2.6.3 KiteVSM_CalcOutput . . . 9

List of Figures

Figure 1. Horseshoe vortices distributed following the convention of the Vortex Step Method (VSM) adopted. A, B are the generic start and end point of the $1/4$-c-bound segment of the generic horseshoe vortex. P is a generic control point located at the $3/4$-c. . . . 1

Figure 2. Representation of Pistolesi's theorem at the generic spanwise wing section. Note the local airfoil coordinate system is displayed. . . . 2

Figure 3. Contribution of the generic *i-th* horseshoe vortex to the induced velocity at the generic P_j. . . . 3

Figure 4. Diagram showing the relative location of of A, B, P_j, P_j' for the trailing-vortex core correction. Other symbols defined in the text. . . . 4

Figure 5. Diagram showing the relative location of A, B, P_j, and P_j'' for the bound-vortex core correction. Other symbols defined in the text. . . . 4

Figure 6. Contribution of the generic *i-th* two-dimensional (2D) bound vorticity to the induced velocity at the generic P_j. . . . 6

List of Tables

List of Acronyms and Symbols

Acronyms

2D	two-dimensional
3D	three-dimensional
AeroDyn	National Renewable Energy Laboratory (NREL)'s aero-hydro-servo-elastic tool for wind turbine design (FAST) aerodynamics module
AeroDyn13	AeroDyn version 13
AeroDyn14	AeroDyn version 14
AeroDyn15	AeroDyn version 15
DS	dynamic stall
FAST	NREL's aero-hydro-servo-elastic tool for wind turbine design
FAST8	FAST version 8
KiteAD	Kite-AeroDyn
KiteFAST	Kite-FAST
KiteVSM	Kite-VSM
MBDYN	MBDYN
NREL	National Renewable Energy Laboratory
VSM	Vortex Step Method

Greek Symbols

$\Gamma(\theta)$	circulation function of spanwise coordinate θ
$\Gamma(y)$	circulation
Γ_i	i-th circulation value
α_G	geometric angle of attack
α_i	induced angle of attack
α_o	Oseen parameter, equal to 1.25643
α_{inc}	angle of incidence
α	angle of attack
δ_f	flap or aileron deflection
δ_y	finite length of the generic bound vortex segment
ε_2	vortex core size for bound vorticity

ε_1	vortex core size
ν	air kinematic viscosity
$\underline{\Gamma}(y)$	circulation vector
$\underline{\Gamma}_i$	i-th circulation vector
$\underline{\eta}_2$	unit vector from the normal projection of P_j'' onto the bound vortex center line to the P_j
$\underline{\eta}$	unit vector from the normal projection of P_j onto the vortex center line to the P_j
$\underline{\xi}$	unit vector along either the relative freestream velocity or the local chord
ρ	air density
θ_a	aero-twist
θ	spanwise coordinate
θ	structural twist deflection plus aero-twist

1 Overview

The dynamics of semi-rigid kites can be simulated by combining models for aerodynamics and structures. This manual describes the theory developed and implemented in Kite-AeroDyn (KiteAD), a new aerodynamics module that works within the MBDYN (MBDYN) framework to simulate airborne wind energy kites.

The main aerodynamic problem for aircraft-like structures winds down to solving for the induction associated with the vorticity field generated by the presence of lifting surfaces. In this document we will call lifting surfaces 'wings', regardless of the actual component function of the surfaces. Various methods exist to accomplish this task, and with various levels of fidelity and computational demand. KiteVSM is based on Weissenger's method (Weissinger 1947), also known as Vortex Step Method (VSM), but with some modifications and extensions to improve the accuracy, computational efficiency, minimization of instabilities and to include the nonlinear airfoil polar data and multiple lift surface contributions.

1.1 VSM Theory Development

The VSM belongs to the vortex-lattice class, and it approximates Prandtl's lifting line theory (Prandtl 1918), with contributions from the work of Munk (stagger theorem Munk 1921), Pistolesi (Pistolesi 1929, $^3/_4$-chord theorem),Wieghardt (Wieghardt 1940), and Mutterperl (Mutterperl 1941). The lifting-line method can be applied to straight, planar wings of high aspect ratio (AR>4). In its original formulation, this method reaches a closed form solution for the induced angle of attack along the wing span by assuming a simple flat plate behavior, where the lift coefficient is simply regarded as $C_l = 2\pi\alpha$.

The VSM, on the other hand, promises accurate solutions for low and high ARs wings of different shape, including swept and dihedral wings. Furthermore, the VSM can be modified to account for the nonlinear polar curve of real airfoils.

Whereas Pradtl's lifting line sheds a continuous trailing vorticity from the wing's $^1/_4$-chord line, the VSM approximates the resulting vortex-sheet with a finite number of horseshoe vortices. The bound portion of the horseshoe vortex lies along the $^1/_4$-c line, with the trailing arms aligned with the freestream direction. One other difference is in the control point locations. The lifting-line calculates induction along control points at the $^1/_4$-c, whereas the VSM places control points at the $^3/_4$-c, but in the direction of the freestream.

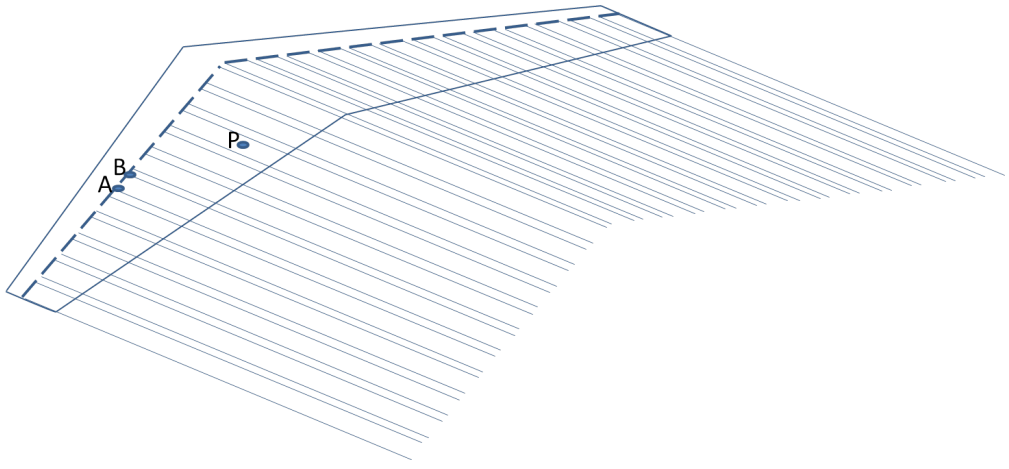

Figure 1. Horseshoe vortices distributed following the convention of the VSM adopted. A, B are the generic start and end point of the $^1/_4$-c-bound segment of the generic horseshoe vortex. P is a generic control point located at the $^3/_4$-c.

Normally, techniques based on Weissenger's method assumes either a simple array of unknown values or some Fourier modal representation with unknown coefficients for the circulation ($\Gamma(y)$=$\Gamma(\theta)$). To attain the unknowns, those methods impose a slip, non-penetration wall condition at the 3/4-c control points, which translates into solving the resulting linear system of equations. The choice of the 3/4-c condition derives from Pistolesi's theorem, which states that the 0-lift angle of attack is approximated by the tangent to the camber line at the 3/4-c location. Therefore, the incidence angle at the 3/4-c point is equal to $\alpha_{inc} = \alpha_G - \arctan\left(\frac{dx}{dy}\Big|_{3/4-c}\right)$ (assuming an airfoil local reference frame).

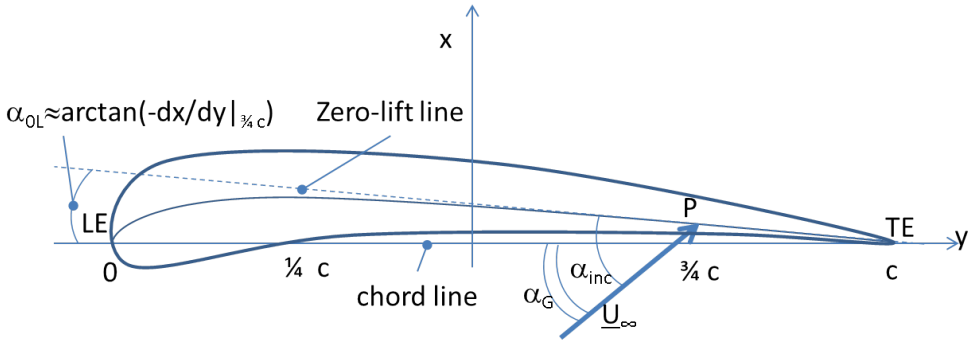

Figure 2. Representation of Pistolesi's theorem at the generic spanwise wing section. Note the local airfoil coordinate system is displayed.

The induced velocity at the control point location (P_j) can be obtained by summing the contributions from all horseshoe vortices with associated circulation $\underline{\Gamma}_i$. The generic induced velocity by the *i-th* horseshoe vortex ($\underline{AB}$, $\underline{A\infty}$, $\underline{B\infty}$) of circulation $\underline{\Gamma}_i$ on the generic P_j can be written, with reference to Fig. 1 and 3, as in Eq. (1.1):

$$\underline{U}_{ind,i}(P_j) = \underline{U}_{AB,i} + \underline{U}_{A\infty,i} + \underline{U}_{B\infty,i} \tag{1.1}$$

where $\underline{U}_{ind,i}(P_j)$ is the induced velocity at the *j-th* P_j by the *i-th* horseshoe vortex $\underline{\Gamma}_i$; $\underline{U}_{AB,i}$ is the contribution to the induced velocity by the i-th bound vorticity segment $\underline{AB}$; $\underline{U}_{A\infty,i}$ is the contribution to the induced velocity by the first trailing-vorticity semi-infinite line of the generic horseshoe vortex $\underline{\Gamma}_i$; $\underline{U}_{B\infty,i}$ is the contribution to the induced velocity by the second trailing-vorticity semi-infinite line of the generic horseshoe vortex $\underline{\Gamma}_i$.

The various terms in Eq. (1.1) can be found by using the Biot-Savart law and can be expressed (ref. Phillips and

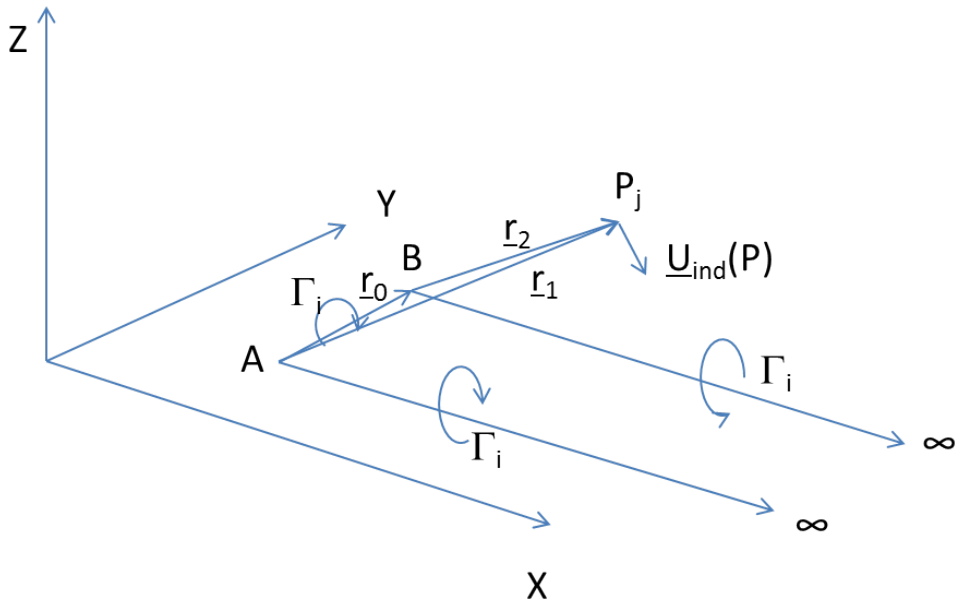

Figure 3. Contribution of the generic *i-th* horseshoe vortex to the induced velocity at the generic P_j.

Snyder 2000) as in Eq. (1.2):

$$
\begin{aligned}
\underline{U}_{AB,i} &= \begin{cases} \dfrac{\Gamma_i}{4\pi}\dfrac{\underline{r}_1\times\underline{r}_2}{|\underline{r}_1\times\underline{r}_2|^2}\left[\underline{r}_0\cdot\left(\dfrac{\underline{r}_1}{r_1}-\dfrac{\underline{r}_2}{r_2}\right)\right] & \text{if} \quad \dfrac{|\underline{r}_1\times\underline{r}_0|}{r_0} > \varepsilon_2 \\ \dfrac{|\underline{r}_1\times\underline{r}_0|}{r_0\varepsilon_2}\underline{U}_{AB,i}(P'_j) & \text{otherwise} \end{cases} \\
\underline{U}_{A\infty,i} &= \begin{cases} \dfrac{\Gamma_i}{4\pi}\dfrac{1+\dfrac{\underline{r}_1\cdot\underline{\xi}}{r_1}}{\left|\underline{r}_1\times\underline{\xi}\right|^2}\underline{r}_1\times\underline{\xi} & \text{if} \quad \left|\underline{r}_1\times\underline{\xi}\right| > \varepsilon_1 \\ \dfrac{\left|\underline{r}_1\times\underline{\xi}\right|}{\varepsilon_1}\underline{U}_{A\infty,i}(P'_j) & \text{otherwise} \end{cases} \\
\underline{U}_{B\infty,i} &= \begin{cases} -\dfrac{\Gamma_i}{4\pi}\dfrac{1+\dfrac{\underline{r}_2\cdot\underline{\xi}}{r_2}}{\left|\underline{r}_2\times\underline{\xi}\right|^2}\underline{r}_2\times\underline{\xi} & \text{if} \quad \left|\underline{r}_2\times\underline{\xi}\right| > \varepsilon_1 \\ \dfrac{\left|\underline{r}_2\times\underline{\xi}\right|}{\varepsilon_1}\underline{U}_{B\infty,i}(P'_j) & \text{otherwise} \end{cases}
\end{aligned}
\tag{1.2}
$$

where $\underline{r}_0$ is the position vector from A to B; $\underline{r}_1$ is the position vector from A to P_j; $\underline{r}_2$ is the position vector from B to P_j; and $\underline{\xi}$ is the unit vector along either the relative freestream velocity or the local chord; the vortex core radius ε_1 for the trailing vorticity is given by Eq. (1.3) (Bhagwat and Leishman 2002) (see also Figure 4):

$$
\varepsilon_1 = \sqrt{4\alpha_o \nu \frac{|\underline{r}_\perp|}{U_\infty}} \tag{1.3}
$$

where ν is the air kinematic viscosity; α_o is the Oseen parameter, equal to 1.25643; and $\underline{r}_\perp$ is the position vector

from either A, B, or C to the projection of P'_j onto the respective vortex centerline as shown in Eq.(1.4):

$$\underline{r}_\perp = (\underline{r}\cdot\underline{\xi})\underline{\xi} \tag{1.4}$$

where $\underline{r}$ is the generic position vector from A, B, or C to P'_j.

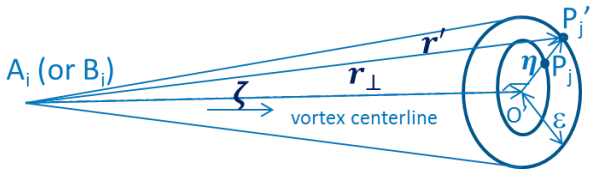

Figure 4. Diagram showing the relative location of of A, B, P_j, P'_j for the trailing-vortex core correction. Other symbols defined in the text.

$\underline{U}_{A\infty,i}(P'_j)$ and $\underline{U}_{B\infty,i}(P'_j)$ are the $\underline{U}_{A\infty,i}$ calculated at the radial projection of P_j on the vortex core edge, $\underline{U}_{A\infty,i}$ calculated at the radial projection of P_j on the vortex core edge, respectively, which can be calculated as in Eq. (1.5):

$$\begin{aligned}
\underline{U}_{A\infty,i}(P'_j) &= \frac{\Gamma_i}{4\pi}\frac{1+\dfrac{\underline{r}'_1\cdot\underline{\xi}}{r'_1}}{\left|\underline{r}'_1\times\underline{\xi}\right|^2}\underline{r}'_1\times\underline{\xi} \\
\underline{U}_{B\infty,i}(P'_j) &= -\frac{\Gamma_i}{4\pi}\frac{1+\dfrac{\underline{r}'_2\cdot\underline{\xi}}{r'_2}}{\left|\underline{r}'_2\times\underline{\xi}\right|^2}\underline{r}'_2\times\underline{\xi} \\
\text{with}\quad \underline{r}' &= \underline{r}_\perp + \varepsilon_1\underline{\eta}
\end{aligned} \tag{1.5}$$

where the $\underline{r}'$ is the position vector from either A or B to P'_j (i.e., either $\underline{r}'_1$ or $\underline{r}'_2$), and the radial unit vector $\underline{\eta}$ can be calculated as in Eq. (1.6):

$$\underline{\eta} = \frac{\dfrac{\underline{r}}{|\underline{r}|}-\underline{\xi}}{\left|\dfrac{\underline{r}}{|\underline{r}|}-\underline{\xi}\right|} \tag{1.6}$$

For the bound vorticity the core radius is fixed as shown in Eq. (1.7) (Garrel 2003) and Figure. 5:

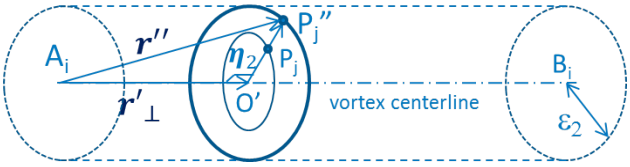

Figure 5. Diagram showing the relative location of A, B, P_j, and P''_j for the bound-vortex core correction. Other symbols defined in the text.

$$\varepsilon_2 = 0.05 * r_0 \tag{1.7}$$

$\underline{U}_{AB,i}(P'_j)$ is the $\underline{U}_{AB,i}$ calculated at the radial projection of P_j on the vortex core edge, which can be calculated as in Eq. (1.8):

$$\begin{aligned} \underline{U}_{AB,i}(P'_j) &= \frac{\Gamma_i}{4\pi} \frac{\underline{r}''_1 \times \underline{r}''_2}{\left|\underline{r}''_1 \times \underline{r}''_2\right|^2} \left[\underline{r}_0 \cdot \left(\frac{\underline{r}''_1}{r''_1} - \frac{\underline{r}''_2}{r''_2}\right)\right] \\ \text{with} \quad & \underline{r}'' = \underline{r}'_\perp + \varepsilon_2 \underline{\eta}_2 \end{aligned} \tag{1.8}$$

where the $\underline{r}''$ is the position vector from either A or B to P''_j (i.e., either $\underline{r}''_1$ or $\underline{r}''_2$), and the radial unit vector $\underline{\eta}_2$ can be calculated as in Eq. (1.9) :

$$\underline{\eta}_2 = \frac{\underline{r}_1 \times \underline{r}_0}{|\underline{r}_1 \times \underline{r}_0|} \tag{1.9}$$

The $\underline{r}'_\perp$ is the position vector from either A, B to the projection of P'_j onto the respective vortex centerline as shown in Eq.(1.10):

$$\underline{r}'_\perp = (\underline{r} \cdot \underline{r}_0) \frac{\underline{r}_0}{r_0^2} \tag{1.10}$$

The typical VSM enforces the slip condition $\underline{U}_{rel} \cdot \underline{n}|_{3/4-c} = 0$ at the $3/4$-c point location on the camber line, i.e.,the thickness is reduced to zero in the approximation of thin airfoils.

In our method, however, we make use of the more generic lifting line fundamental equation as in Eq. (1.11) (e.g., Anderson 2001) to create a constraint (**f**=$\underline{0}$) for the circulation distribution $\Gamma(y)$:

$$\mathbf{f} = \rho \left|\underline{U}_\infty \times \underline{\Gamma}(y)\right| - \frac{1}{2}\rho \left|\underline{U}_{rel} \times \hat{z}_{airf}\right|^2 c C_l\left(\alpha, \delta_f\right) = 0 \tag{1.11}$$

where ρ is the air density; $\underline{U}_\infty$ is the Free-stream air velocity vector; $\underline{\Gamma}(y)$ is the circulation vector; $\underline{U}_{rel}$ is the relative air velocity; $\hat{z}_{airf}$ is the unit vector along the airfoil z-axis; c is the chord length; $C_l\left(\alpha, \delta_f\right)$ is the 2D lift coefficient as a function of α and δ_f; α is the effective angle of attack seen by the airfoil; δ_f is the airfoil's flap or aileron deflection; $\underline{k}$ is the unit vector normal to the relative velocity. The nonlinearity stems from $C_l\left(\alpha, \delta_f\right)$, and from the U_{rel}^2 term. Eq. (1.11) represents an array of constraints, one per i-th element in the VSM model ($i = 1..N_{elms}$).

In Eq. (1.11), the unknowns are $\underline{\Gamma}(y)$, U_{rel}, and α. The latter two can be expressed as a function of the induced velocity and thus $\underline{\Gamma}(y)$.

$$\begin{aligned} \underline{U}_{rel} &= \underline{U}_\infty + \underline{U}_{ind} \\ \underline{U}_{ind}(P_j) &= \sum_i \underline{U}_{ind,i}(P_j) = \sum_i \left[\underline{U}_{AB,i} + \underline{U}_{A\infty,i} + \underline{U}_{B\infty,i}\right] \\ \alpha &= \arctan \frac{\underline{U}_{rel} \cdot \hat{x}_{airf}}{\underline{U}_{rel} \cdot \hat{y}_{airf}} \end{aligned} \tag{1.12}$$

where $\underline{U}_{rel}$ is the relative air velocity; $\underline{U}_{ind}$ is the induced velocity ; $\hat{x}_{airf}$ is the unit vector along the airfoil x-axis; $\hat{y}_{airf}$ is the unit vector along the airfoil y-axis.

Eq. (1.11) has the great advantage of incorporating the generic polar curve of an airfoil through $C_l\left(\alpha, \delta_f\right)$, thus accounting for nonlinear effects of actual airfoils (beyond the simple flat plate of the lifting line method) and for the presence of flap or moving surface deflections. Other methods are proposed in the literature to account for nonlinear polars, but introduce more complications with multiple solving loops and with mixed success (Dam, Vander Kam, and Paris 2001; Ortega, M., and Komatsu 2004).

Our innovative method, however, does not converge to the correct solution as it is written. The reason is that Eq. (1.11) in the lifting-line sense should be enforced at the 1/4-c, whereas we are using the 3/4-c control point location to account for the effects of camber. In order to bring the solution back on track, we must account for the effect of a 2D contribution to the induction. The new induced velocity is calculated as in Eq. (1.13), which leverages some of the works by Piszkin and Levinsky 1976; Ranneberg 2015:

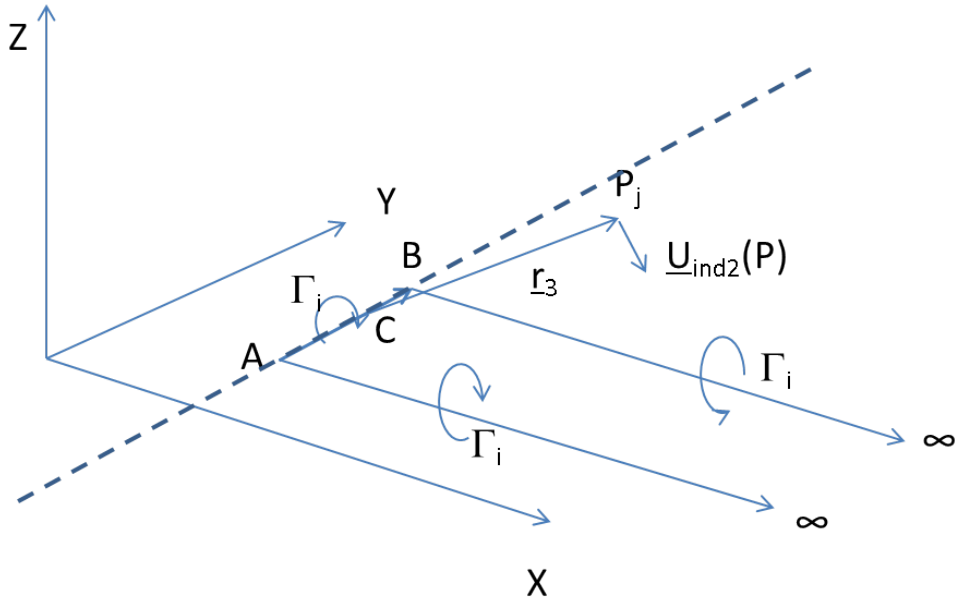

Figure 6. Contribution of the generic *i-th* 2D bound vorticity to the induced velocity at the generic P_j.

$$\underline{U}_{ind,i}(P_j) = \underline{U}_{AB,i} + \underline{U}_{A\infty,i} + \underline{U}_{B\infty,i} - \underline{U}_{AB2D,ij} \tag{1.13a}$$

$$\underline{U}_{AB2D,ij} = \begin{cases} \frac{\Gamma_i}{2\pi} \frac{\underline{r}_0 \times \underline{r}_3}{|\underline{r}_0 \times \underline{r}_3|^2} r_0 \delta_{ij} \end{cases} \tag{1.13b}$$

where $\underline{r}_3$ is the position vector from C (midpoint of $\underline{AB}$) to P_j; $\underline{U}_{AB2D,ij}$ is the contribution to the induced velocity by the 2D bound vorticity aligned with the segment $\underline{AB}$ and it is considered only for control point within the local vortex element; δ_{ij} is the Kronecker's delta, equal to 0 unless $i = j$, in which case it is equal to 1.

The induced velocity is therefore calculated as the difference between a three-dimensional (3D) and a 2D contribution. By doing so, Eq. (1.11) can be enforced at each control point where U_{rel}, α, and $C_l\left(\alpha, \delta_f\right)$ are expressed in terms of Γ_i. The resulting nonlinear system of equations can then be solved with a numerical method, e.g.,Newton's solver.

$$\underline{U}_{ind}\left(P_j\right) = \sum_{i=1}^{N_{elms}} \underline{U}_{ind,i}(P_j) = \sum_{i=1}^{N_{elms}} \left[\underline{U}_{AB,i} + \underline{U}_{A\infty,i} + \underline{U}_{B\infty,i} - \underline{U}_{AB2D,ij}\right] \tag{1.14}$$

The presence of multiple lifting surfaces is simply given by the superposition of the induced velocities (see Eq. (1.14), which replaces the second in Eq. (1.12)), i.e.,the induced velocity at the generic P_j is calculated the same way as in Eq. (1.13), where the contribution of each $i-th$ horseshoe vortex must be taken into account from all lifting surfaces.

Enforcing Eq. (1.11) at each control point (one per horseshoe vortex) renders a system of nonlinear equations, where the various terms can be calculated as a function of $\underline{\Gamma}(y)$ as shown in Eq. (1.12) and Eq. (1.13), with $C_l\left(\alpha, \delta_f\right)$ calculated from an interpolation of the airfoil polar data.

1.2 KiteVSM additional theory

The VSM is the base tool to calculate the distribution of lift along the wing span. MBDYN, however, will require a set of loads at the various nodes (C) along the wings.

With reference to Figure 2, the calculation of shear forces and torque moment (pitching moment) at each spanwise station is done as follows:

- with local values of U_{rel}, α, c, δ_y (finite length of the generic bound vortex segment) calculate:

$$F_x = 0.5 \cdot \rho U_{rel}^2 c \delta_y \left[C_l\left(\alpha, \delta_f\right) \cdot \cos\alpha + C_d\left(\alpha, \delta_f\right) \cdot \sin\alpha \right] \tag{1.15}$$

$$F_y = 0.5 \cdot \rho U_{rel}^2 c \delta_y \left[-C_l\left(\alpha, \delta_f\right) \cdot \sin\alpha + C_d\left(\alpha, \delta_f\right) \cdot \cos\alpha \right] \tag{1.16}$$

$$M_z = 0.5 \cdot \rho U_{rel}^2 c^2 \delta_y \cdot C_m\left(\alpha, \delta_f\right) \tag{1.17}$$

where $C_l\left(\alpha, \delta_f\right)$, $C_d\left(\alpha, \delta_f\right)$, $C_m\left(\alpha, \delta_f\right)$ are given by interpolation of the airfoil tables (AFI_{Params}). Note that these forces and moments are considered applied at the $^1/_4$-c points.

2 Implementation Algorithm

Here is a suggested approach to the algorithm implementation within FAST version 8 (FAST8).

2.1 Inputs, Outputs, Parameters, States

2.1.1 Init_Inputs

Beside the standard variables common to all modules ($OutFmt$, $OutSFmt$, $NumOuts$, $OutList$), the Init_Inputs to the KiteVSM are:

- VSM_{mod} –flag indicating whether control points and trailing vortices are aligned along the chord (1) or the local free stream direction (2) DOES THIS ONE GO IN TO KiteAD?
- δ_y: finite length of the generic bound vortex segment per element
- c: chord length per wing element
- $AFidx$: index pointing to the correct airfoil file/table/database per wing element
- θ_a: per wing element

Do all the calculations the first time CalcOutput is called setting a temporary variable that mimics the sate.

2.2 Inputs u

The Inputs to the KiteVSM are:

- $\underline{U}_\infty$: Free-stream air velocity vector. What is really needed are the components in the plane of the local element airfoil (x, y), including contributions from structural body motions and wind velocity.
- A,B coordinates for every element, in the aircraft reference frame (O, x_b, y_b, z_b). From these, the local chord length, and the $\underline{U}_\infty$, the C and P coordinates can be calculated.
- θ: structural twist deflection plus aero-twist per wing element
- δ_f: flap or aileron deflection (control setting per blade element)

Note: these are for a given node (within a given lifting surface) and chord. Density is used to calculate the dimensional load at each spanwise station. U_∞ should include the body motion.

2.3 Outputs y

The Outputs from the KiteVSM are:

- F_x: shear force along the airfoil's x-axis, at each spanwise station y
- F_y: shear force along the airfoil's y-axis, at each spanwise station y
- M_z: torque moment about the lifting surface z-axis, at each spanwise station y

The outputs are calculated via Eqs. (1.15)–(1.17), and using Eqs. (1.12) with the calculated state Γ_i.

2.4 States x_z

The states for KiteVSM are constraint states:

- $\Gamma(y)$: circulation

Note: perhaps normalizing $\Gamma(y)$ by the local $\underline{U}_\infty$ could reduce errors in the residual within the *CalcOutput* calculations where the new time step $\underline{U}_\infty$ will be used.

2.5 Parameters p

The Parameters for the KiteVSM are:

- VSM_{mod} –flag indicating whether control points and trailing vortices are aligned along the chord (1) or the local free stream direction (2) DOES THIS ONE GO IN TO KiteAD?
- δ_y: finite length of the generic bound vortex segment per element
- c: chord length per wing element
- θ_a: per wing element
- AFI_{Params}: airfoil static tables of C_l C_d C_m and dynamic stall (DS) parameters
- $AFidx$: index pointing to the correct airfoil file/table/database
- ν: air kinematic viscosity

2.6 Kite-VSM Implementation

2.6.1 KiteVSM_Init Routine

This routine allocates the module's data structures, initializes the module's states, and sets the non-time-varying parameters (copies them from the initialization input data section) (see also Section 2.1.1).

- $\Gamma(y)(0)$= elliptical distribution

2.6.2 KiteVSM_UpdateStates Routine

For a given set of inputs (u), and at the current step in time (t_i):

- use the current time step $\Gamma(y)_i$ as initial guess to solve for $\Gamma(y)_{i+1}$ by numerically solving Eq. (1.11), together with Eqs. (1.2), (1.13), and (1.12). Inputs will come in at t_{i+1}

2.6.3 KiteVSM_CalcOutput

By using Eqs.(1.15)–(1.17), calculate:

- F_x: shear force along the airfoil's x-axis, at each spanwise station y
- F_y: shear force along the airfoil's y-axis, at each spanwise station y
- M_z: torque moment about the lifting surface z-axis, at each spanwise station y

The outputs are calculated via Eqs. (1.15)–(1.17), and using Eqs. (1.12) with the calculated state Γ_i through Eqs. (1.2), (1.5), (1.8), (1.13), and (**??**).

Bibliography

Anderson, J. D. Jr. 2001. *Fundamentals of Aerodynamics*. 3rd. McGraw-Hill Series in Aeronautical and Aerospace Engineering. McGraw-Hill.

Bhagwat, M. J., and J. G. Leishman. 2002. "Generalized Viscous Vortex Model for Applications to Free-Vortex Wake Aeroacoustic Calculations". In *58th Annual Forum and Technology Display of the American Helicopter Society International*. Montreal, Canada.

Dam, C. P. van, J. C. Vander Kam, and J. K. Paris. 2001. "Design-Oriented High-Lift Methodology for General Aviation and Civil Transport Aircraft". *J. of Aircraft* 38 (6): 1076–1084.

Garrel, A. van. 2003. *Development of a Wind Turbine Aerodynnamics Simulation Module*. Tech. rep. ECN-C–03-079. The Netherlands: ECN.

Munk, M. M. 1921. *The Minimum Induced Drag of Aerofoils*. Tech. rep. NACA-TR-121. Washington, DC: National Advisory Committee for Aeronautics.

Mutterperl, W. 1941. *The Calculation of Span Load Distributions of Swept-back Wings*. Tech. rep. NACA-TN-834. Washington, DC: National Advisory Committee for Aeronautics.

Ortega, M. A., Girardi. R. M., and P. S. Komatsu. 2004. "A Numerical Method to Predict the Lift of Aircraft Wings at Stall Conditions". In *ENCIT 2004 – ABCM*. Rio de Janeiro, Brazil.

Phillips, W. F., and D. O. Snyder. 2000. "Modern Adaption of Prandtl's Classic LLifti-Line Theory". *J. of Aircraft* 37 (4): 600–608.

Pistolesi, E. 1929. *Alcune considerazioni sul problema del biplano indefinito*. Tech. rep. Rome University.

Piszkin, S. T., and E. S. Levinsky. 1976. *Nonlinear Lifting Line Theory for Predicting Stalling Instabilities on Wings of Moderate Aspect Ratio*. Tech. rep. CASD-NSC-76-001. 5001 Kearny Villa Rd., San Diego, CA 92138: General Dynamics Convair Division.

Prandtl, L. 1918. *Theory of Lifting Surfaces*. Tech. rep. NACA-TR-116. Washington, DC: National Advisory Committee for Aeronautics.

Ranneberg, M. 2015.

Weissinger, J. 1947. *The Lift Distribution of Swept-Back Wings*. Tech. rep. NACA-TM-1120. Langley Aeronautical Lab., Langley Field, VA: National Advisory Committee for Aeronautics.

Wieghardt, K. 1940. *Chordwise Load Distribution of a Simple Rectangular Wing/WinLoad*. Tech. rep. NACA-TM-963. Washington, DC: National Advisory Committee for Aeronautics.